

Optical property measurements of lithium chloride aqueous solution for a novel solar neutrino experiment

Ye Liang,^{1, 2,*} Tong Xu,^{1, 2} Jialiang Zhang,³ Ming Qi,³ and Zhe Wang^{1, 2, 4, †}

¹*Department of Engineering Physics, Tsinghua University, Beijing 100084, China*

²*Center for High Energy Physics, Tsinghua University, Beijing 100084, China*

³*School of Physics, Nanjing University, Nanjing 210093, China*

⁴*Key Laboratory of Particle & Radiation Imaging (Tsinghua University), Ministry of Education, Beijing 100084, China*

(Dated: November 18, 2022)

The lithium chloride aqueous solution has a great potential to be the detection medium of a novel solar neutrino detector, for the nuclide ${}^7\text{Li}$ provides a charged-current interaction channel with a high cross-section for the MeV-scale solar electron-neutrinos, enabling measurement of solar neutrino spectrum. Previous research questioned the optical transparency of the lithium chloride solution for building a large detector. This work measures the optical properties of a saturated lithium chloride solution. The solution shows no interfering fluorescence or absorption in the UV/visible wavelength range. The attenuation length is measured to be 10.9 ± 0.2 m. Also measured is the Cherenkov light yield of the lithium chloride solution. This work shows that the lithium chloride aqueous solution does not obstruct the propagation of the Cherenkov light and it is feasible in the sense of optical transparency to use a saturated lithium chloride solution to build a neutrino detector with a size of 10 meters.

I. INTRODUCTION

The measurements of solar neutrinos [1–5] have triggered the study of neutrino mixing and oscillation and reveal the knowledge of the solar model. New experiments [6–8] are proposed to further improve the measurement of solar neutrino oscillation and solar model.

The nuclide ${}^7\text{Li}$ is an attractive candidate for the MeV-scale neutrino target [9–12]. The reaction $\nu_e + {}^7\text{Li} \rightarrow e^- + {}^7\text{Be}$ provides a measurement of solar neutrino energy spectrum through a reaction of $E_{\nu_e} = E_T + 0.862 \text{ MeV}$. E_T is the kinetic energy of electron and the last value is the threshold of the neutrino charged-current (CC) channel on ${}^7\text{Li}$ [9]. The total CC cross section of ${}^8\text{B}$ solar neutrino is $3.5 \times 10^{-42} \text{ cm}^2$, nearly 60 times that of the neutrino elastic scattering on electrons [9]. The energy of the emitted electron well reflects the energy of the incident neutrino. The direction of the electron is close to uniform, which can help distinguish the CC interactions from the elastic scatterings.

Lithium chloride is highly soluble in water, 82.8 g/100 g at 20 °C, i.e. (45.29%w/w) [13]. The compound is cost-effective, neutral, and nontoxic, and its aqueous solution is readily accessible. But the previous attempt by SUNLAB mentioned in Haxton [10] of making a practical Cherenkov detector with LiCl aqueous solution was severely hindered by a lack of optical transparency, especially in the UV. Instead, LiOH was suggested by Haxton [10], which is alkaline and is of much less water-solubility than LiCl. The preparation and the measurement details were not published by SUNLAB.

This work demonstrates that saturated LiCl solution is capable being a Cherenkov detecting medium. Section II describes the LiCl solution preparation with microfiltration and adsorption. The absorption and fluorescence emission spectra of the purified solution and the measured attenuation length with a long tube are shown in section III. The Cherenkov light yield of LiCl solution is compared with water with a device using cosmic-ray muons in section IV.

II. PREPARATION

Like any other alkali metal chloride, LiCl salt is odorless, inflammable, and nontoxic; it is insensitive to acidity variation and is chemically stable in most cases.

* Corresponding author: liangy20@mails.tsinghua.edu.cn

† Corresponding author: wangzhe-hep@tsinghua.edu.cn

Industrial-grade LiCl contains ppm to ppb level impurities, in which ferric salt predominates. These impurities impair optical transparency. Microfiltration can conveniently remove insoluble and colloidal impurities, such as that in Ref. [14]. Powdered activated carbon (PAC) is commonly used to remove organic impurities by adsorption.

In this study, LiCl powder of 99% purity is purchased from Shanghai Aladdin Biochemical Technology Co., Ltd. High purity deionized water with $18.2 \text{ M}\Omega \text{ cm}^{-1}$ is produced with a pure water machine from Zhongyang company. All the glass containers are cleaned by ultrasonics with a detergent solution at 60°C for half an hour and then rinsed with a large quantity of pure water.

To make a saturated solution, an excessive amount of LiCl is dissolved into pure water with a vigorous stir. The solution is then vacuum-filtered twice. The first filtration uses a piece of cellulose acetate membrane with a pore size of $0.22 \mu\text{m}$, and the second uses $0.10 \mu\text{m}$. After the filtrations, the solution becomes homogeneous, colorless, and transparent. PAC is used to further remove any possible organic impurities which may undermine the transparency in the UV, followed by a second $0.10 \mu\text{m}$ filtration. The saturated LiCl solution is measured to have a density of $1.27 \pm 0.01 \text{ g/mL}$ and a concentration of $45.16 \pm 0.01\% \text{ w/w}$ at 20°C .

III. MEASUREMENTS OF OPTICAL PROPERTIES

A. Fluorescence Spectrum

The fluorescence of purified LiCl solution is measured by a Lengguang Tech. F97Pro fluorospectrometer. The excitation wavelength is scanned from 200 nm to 800 nm. For each excitation wavelength, the emission intensity is measured in the same wavelength range. A sample of linear alkylbenzene (LAB) is also scanned as a reference, which is known as a typical solvent of organic liquid scintillator and has weak fluorescence. The measurements for the two samples use the same gain of the photosensor and scan settings. Three-dimensional fluorescence spectra are shown in Fig. 1.

Fig. 1(a) is the spectrum for the LiCl solution. Fig. 1(b) shows a typical fluorescence peak of LAB around the excitation of 320 nm and the emission of 340 nm. Compared to the spectrum of LAB, Fig. 1(a) shows no sign of fluorescence for the LiCl solution. The variance of the signals in the spectrum of LiCl solution is around 0.01% of that of LAB, which should be attributed to the fluctuation of the spectrophotometer. This property is intuitive since this inorganic solution has no fluorophore, such as the benzene ring in LAB.

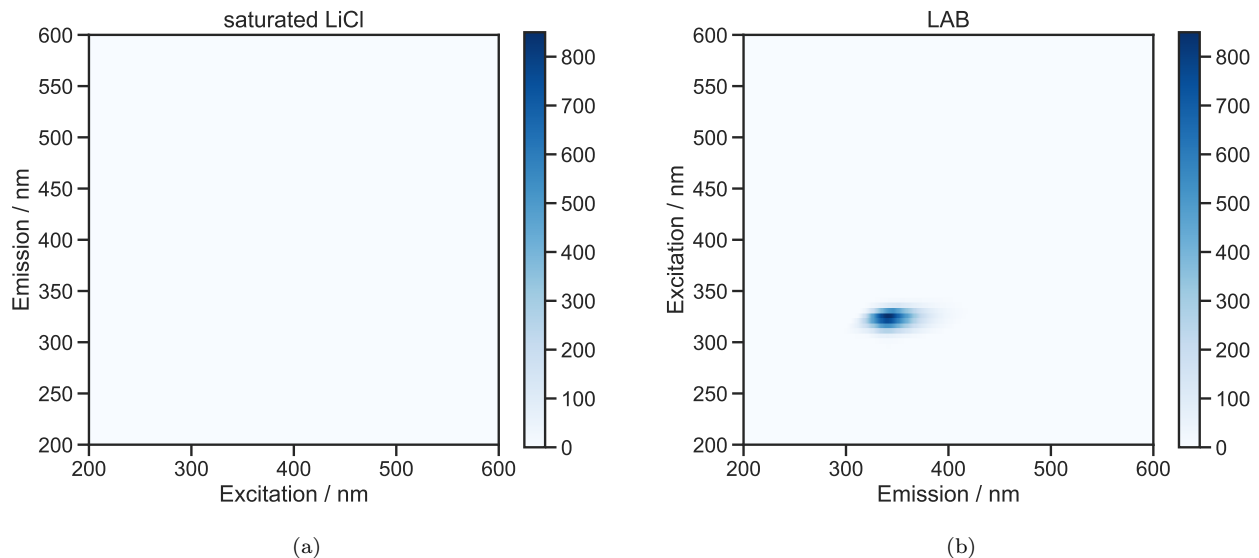


FIG. 1. Three-dimensional fluorescence spectra of (a) the saturated LiCl solution and (b) a linear alkylbenzene reference.

B. Absorption Spectrum

The absorption of LiCl is measured by a Persee TU-1901 spectrophotometer. A 10 cm quartz cuvette is used, and the air is used as blank. The absorbance is defined as

$$A = -\log_{10} \frac{I}{I_0}, \quad (1)$$

where I_0 is the intensity of the incident light, and I is that of the transmitted light. Fig. 2 shows the absorption spectra of saturated LiCl solution with and without the treatment with PAC. The spectrum of pure water is shown for comparison. The saturated LiCl shows little absorption higher than water between 300 nm to 550 nm, which matches the sensitive region of typical bialkali photomultiplier tubes (PMTs) used in neutrino detectors. The use of PAC is shown to be effective for purification.

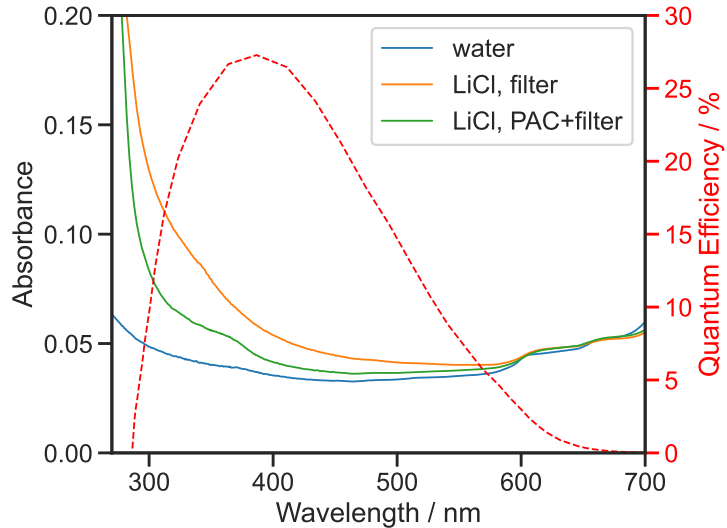


FIG. 2. UV-vis absorption spectra of the saturated LiCl solution and pure water. Filter indicates that the solution is filtered with a $0.10\text{ }\mu\text{m}$ membrane, while filter+PAC indicates that the solution is treated with powdered activated carbon and then $0.10\text{ }\mu\text{m}$ filtration. A 10 cm cuvette is used. The quantum efficiency spectrum of a typical bialkali PMT [15] is shown as a reference.

C. Attenuation Length Measurement

The attenuation length of a saturated LiCl solution after purification is measured with a tubular system, shown in Fig. 3. The apparatus is built based on the attenuation length measurement system that measures the attenuation lengths of liquid scintillators for Daya Bay and JUNO neutrino experiments [16–19]. The stainless steel tube in the original apparatus is replaced with a polyvinyl chloride (PVC) tube in this work to prevent galvanic corrosion. The PVC tube is 0.84 m long and has an inner radius of 3.36 cm. The inner surface of the tube is black to reduce the reflection. The bottom of the tube is sealed with a thin piece of quartz transparent to UV light. The light source on the top is a 430 nm light-emitting diode (LED, emission spectrum shown in Fig. 4), controlled by a high-frequency signal generator. A pulse of light, emitted at a frequency of 800 Hz and collimated by a lens and a diaphragm, passes through the liquid in the tube and the quartz piece, and finally sheds onto a 2-inch Hamamatsu R7724 bialkali PMT. The light spot is around 1.5 mm in diameter and right in the center of the photocathode. After the trigger from the signal generator, which is synchronized with the LED emission, the PMT signal is read out by a CAEN V965 charge-to-digital converter [20], converted to an analog-to-digital-conversion (ADC) value, which is proportional to the intensity of the transmitted light. The path length of the light through the liquid can be adjusted by the valve on the side. The whole apparatus is placed inside a dark box, grounded to shield the

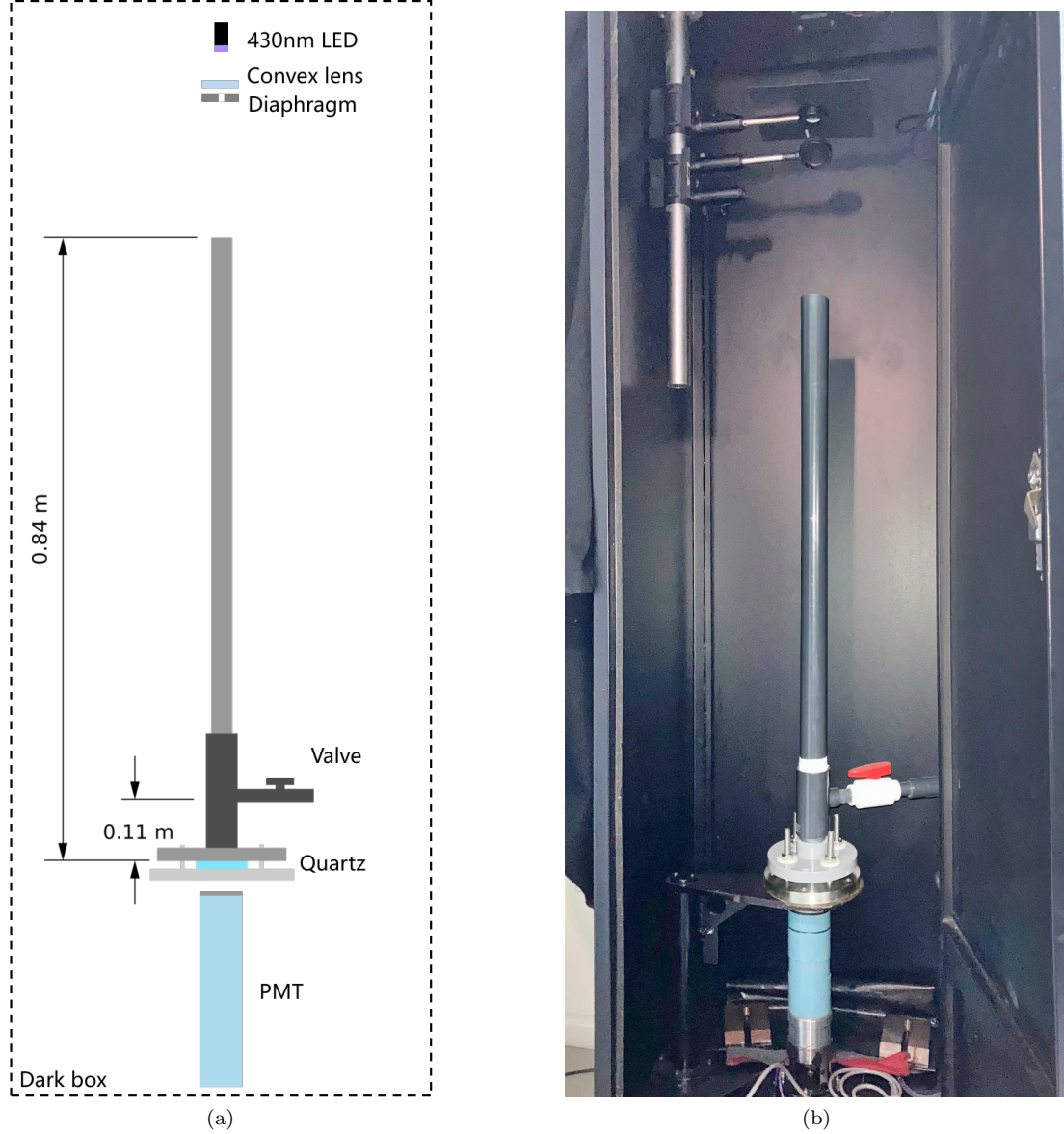


FIG. 3. The tubular system for attenuation length measurement. (a) A sketch and (b) a photo of the system.

electromagnetic interference. The box and the controlling system are placed in a dark room to reduce stray light. The environmental temperature is controlled to fluctuate less than 0.2°C during the measurement.

In the measurement of the attenuation length of the LiCl solution, the path length varies from 0.79 m to 0.14 m. The error of the path lengths is estimated to be 1 cm, which predominates the system error. For each path length, the data taking persists 2 minutes to obtain around 40,000 measurements of ADC values. Then a Gaussian fit is used to determine their mean value and error.

The attenuation length is obtained by fitting an exponential as shown in Fig. 5. The attenuation length is measured to be 10.9 ± 0.2 m for the light of 430 nm.

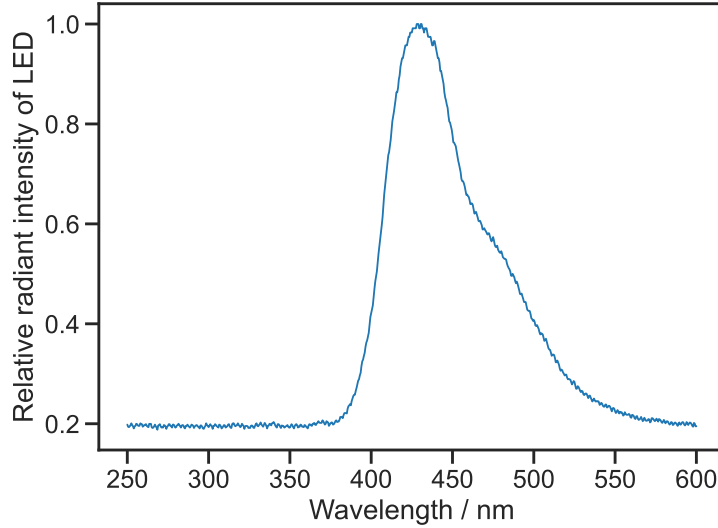


FIG. 4. Emission spectrum of the LED used in the tubular apparatus for attenuation length measurement.

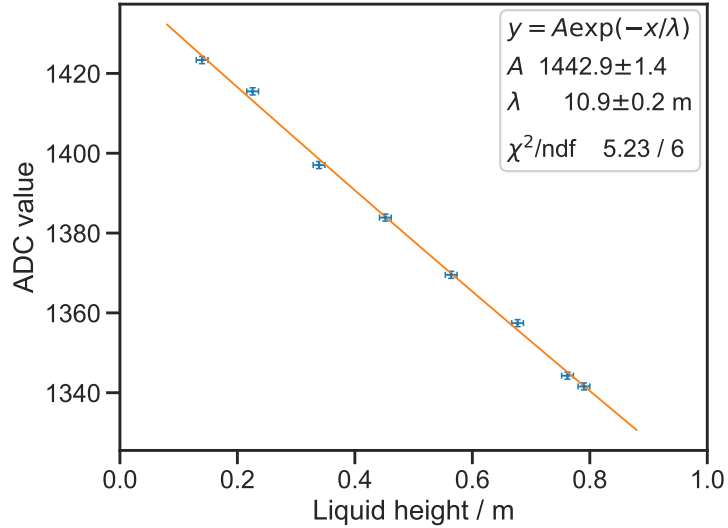


FIG. 5. Exponential fitting result of light attenuation in the LiCl solution.

IV. CHERENKOV LIGHT YIELD VERIFICATION

A. Experiment

The LiCl solution does not hinder the propagation of Cherenkov light is verified by measuring the Cherenkov light yield of the solution with a cosmic ray muons telescope (Fig. 6). The device was used for the search of slow liquid scintillators [21, 22]. It comprises a 15.4 L acrylic tank, four plastic coincidence scintillators, two anti-coincidence scintillators, and a pair of measuring PMTs. The tank is the container of the detecting medium. The inner surface is painted black and granulated to reduce the reflection. Four coincidence scintillators are used to trigger the

data acquisition system when a cosmic ray muon is detected passing through the tank from top to bottom. The anti-coincidence scintillators on the side are used to tag the shower events that will be rejected later in the offline analysis. The measuring PMTs are two 2-inch Hamamatsu R1828-01 bialkali PMTs, which are mounted on the top and bottom of the detector tank. Their glass heads are slightly immersed in the liquid medium to avoid additional refraction. When a muon downwardly shoots into the medium, the bottom PMT measures the Cherenkov signals, while the top PMT detects the scintillation and reflection, if any. A CAEN VX1721 flash analog-to-digital converter [20] is used to process the trigger and read out the waveforms.

Predominant noises are electronic noises and multi-muon events. The former are removed by checking the peak-to-charge-ratio and peak-to-width-ratio of their waveforms. The latter are removed by first checking if any signal is presented in the anti-coincidence channels, and then checking if the integrated charges in the coincidence channels deviate from a Landau distribution. Around 1,000 events are obtained in the measurement for each sample. The average waveforms of the top and the bottom PMT are shown in Fig. 7, respectively. The bottom PMT receives significant Cherenkov signals, while the top PMT receives tiny signals at the same time, which should be the effect of reflection. The charge Q of the waveform can be calculated by integrating within the time interval from 10 ns before the peak to 10 ns after the peak. Then the Cherenkov photoelectron (PE) number of the bottom PMT is calculated with

$$N_{\text{PE}} = \frac{Q}{Q_{\text{SPE}}} \quad (2)$$

where Q_{SPE} is the gain of the PMT, which is calibrated using the single-photoelectron signals of dark noise. The error from the calculation of integrated charge is estimated by including the ringing of the waveform, which is around 10%. The error caused by reflection is estimated by integrating the waveform of the top PMT, which is around 3%. The statistical error from PMT gain calibration is around 5%. The total error is then 12%.

In this work, the Cherenkov PE yield of a purified, saturated LiCl solution is measured. The Cherenkov PE yield of pure water is also measured for comparison. The results are shown in Table I. The Cherenkov light yields of the LiCl solution and pure water are in agreement within the error range of 1σ .

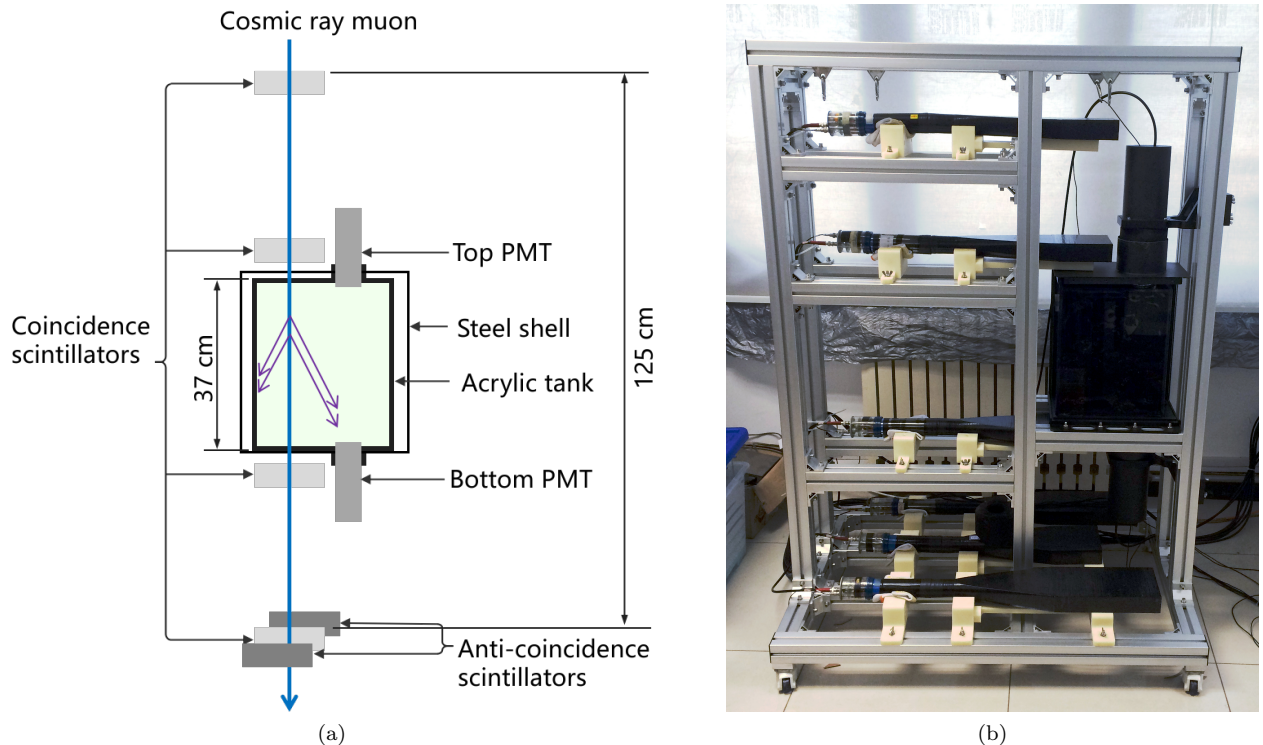


FIG. 6. The cosmic ray muon telescope for Cherenkov light yield measurement. (a) A sketch and (b) a photo.

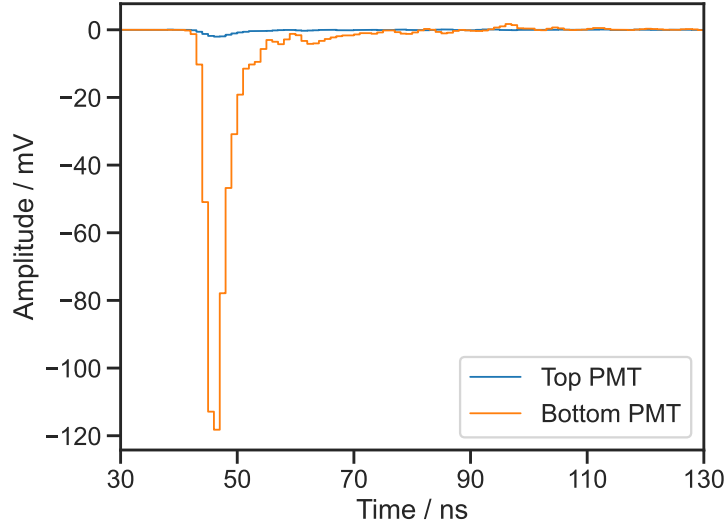


FIG. 7. The average waveforms from the top and the bottom PMT of the muon telescope for the LiCl solution.

TABLE I. Cherenkov light yields per muon event in saturated lithium chloride solution and in pure water. Monte Carlo simulation result of a water detector is also listed.

Detecting medium	Cherenkov PE number
Saturated LiCl solution	10.03 ± 1.2
Pure water	10.28 ± 1.2
Simulation using water	9.5 ± 1.1

B. Comparison with Simulation

A Monte Carlo simulation based on GEANT4 [23–25] is implemented to verify the experiment results. In the simulation, the detector tank with water as is in the experiment is constructed and the top and the bottom PMT are placed. The energy of the incident muon is sampled with a power law distribution with an order of -2.7 , which is the low energy asymptote of the Gaisser formula [26]. Standard electromagnetic and muon-nucleus processes are included. The refraction indices of water for different wavelengths are set according to Ref. [27]. Around 7,000 muon events with Cherenkov signals are obtained in the simulation. The effect of reflection predominates the error, which is estimated to be around 10%. The result shows that on average 9.5 ± 1.1 Cherenkov PE is captured by the bottom PMT for each event. This is in agreement with the experiment results.

V. SUMMARY AND CONCLUSION

Cherenkov detector with highly concentrated lithium salt is an attractive candidate for MeV-scale solar neutrino detection. This work measures the optical properties of a saturated LiCl solution to reveal its potential for making up a neutrino detector. The purified LiCl solution shows no fluorescence and almost no absorption in the sensitive range of common bialkali PMTs. The attenuation length is measured to be 10.9 ± 0.2 m, which is a contradictory evidence against the claim in Ref. [10]. The Cherenkov light yield of the solution is measured using a cosmic ray muon telescope. The experiment shows that the Cherenkov light induced by cosmic ray muons is consistent with pure water with the current setup. In conclusion, the saturated LiCl solution is demonstrated optically good for a Cherenkov detector with a size of ten meters.

VI. ACKNOWLEDGEMENT

This work is supported in part by the National Natural Science Foundation of China (Nos. 12141503 and 11620101004), the Ministry of Science and Technology of China (No. 2018YFA0404102), the Key Laboratory of Particle & Radiation Imaging (Tsinghua University), and the CAS Center for Excellence in Particle Physics (CCEPP).

[1] R. Davis, “A review of the homestake solar neutrino experiment,” *Progress in Particle and Nuclear Physics* **32**, 13 (1994), ISSN 0146-6410, [http://dx.doi.org/10.1016/0146-6410\(94\)90004-3](http://dx.doi.org/10.1016/0146-6410(94)90004-3).

[2] N. Ferrari, J. C. Lanfranchi, and L. Pandola, “The GNO experiment,” *Nuclear Physics B - Proceedings Supplements* **143**, 560 (2005), ISSN 0920-5632, <http://dx.doi.org/10.1016/j.nuclphysbps.2005.01.225>.

[3] D. Vignaud, “The GALLEX solar neutrino experiment,” *Nuclear Physics B - Proceedings Supplements* **60**, 20 (1998), ISSN 0920-5632, [http://dx.doi.org/10.1016/S0920-5632\(97\)00498-2](http://dx.doi.org/10.1016/S0920-5632(97)00498-2).

[4] S. Fukuda, *et al.*, “The Super-Kamiokande detector,” *Nuclear Instruments and Methods in Physics Research Section A: Accelerators, Spectrometers, Detectors and Associated Equipment* **501**, 418 (2003), ISSN 0168-9002, [http://dx.doi.org/10.1016/S0168-9002\(03\)00425-X](http://dx.doi.org/10.1016/S0168-9002(03)00425-X).

[5] J. Boger, *et al.*, “The Sudbury Neutrino Observatory,” *Nuclear Instruments and Methods in Physics Research Section A: Accelerators, Spectrometers, Detectors and Associated Equipment* **449**, 172 (2000), ISSN 0168-9002, [http://dx.doi.org/10.1016/S0168-9002\(99\)01469-2](http://dx.doi.org/10.1016/S0168-9002(99)01469-2).

[6] F. D. Lodovico, “The Hyper-Kamiokande Experiment,” *J. Phys.: Conf. Ser.* **888**, 012020 (2017), ISSN 1742-6596, <http://dx.doi.org/10.1088/1742-6596/888/1/012020>.

[7] T. Adam, *et al.*, “JUNO conceptual design report,” *ArXiv Prepr. ArXiv:1508.07166* (2015), <http://dx.doi.org/10.48550/arXiv.1508.07166>.

[8] J. F. Beacom, *et al.*, “Physics prospects of the Jinping neutrino experiment,” *Chinese Phys. C* **41**, 023002 (2017), ISSN 1674-1137, <http://dx.doi.org/10.1088/1674-1137/41/2/023002>.

[9] J. N. Bahcall, *Neutrino Astrophysics* (Cambridge University Press, 1989).

[10] W. C. Haxton, “Salty Water Cerenkov Detectors for Solar Neutrinos,” *Phys. Rev. Lett.* **76**, 4 (1996), <http://dx.doi.org/10.1103/PhysRevLett.76.1562>.

[11] J. R. Alonso, *et al.*, “Advanced Scintillator Detector Concept (ASDC): A Concept Paper on the Physics Potential of Water-Based Liquid Scintillator,” *ArXiv Prepr. ArXiv:1409.5864* (2014), <http://dx.doi.org/10.48550/arXiv.1409.5864>.

[12] W. Shao, *et al.*, “The Potential to Probe Solar Neutrino Physics with LiCl Water Solution,” *ArXiv Prepr. ArXiv:2203.01860* (2022), <http://dx.doi.org/10.48550/arXiv.2203.01860>.

[13] J. Kwan, *CRC Handbook of Chemistry and Physics* (CRC Press, 2020).

[14] M. Yeh, J. B. Cumming, S. Hans, and R. L. Hahn, “Purification of lanthanides for large neutrino detectors: Thorium removal from gadolinium chloride,” *Nuclear Instruments and Methods in Physics Research Section A: Accelerators, Spectrometers, Detectors and Associated Equipment* **618**, 124 (2010), ISSN 0168-9002, <http://dx.doi.org/10.1016/j.nima.2010.02.124>.

[15] “Hamamatsu Photonics,” <https://www.hamamatsu.com/>.

[16] G. Yu, *et al.*, “Some new progress on the light absorption properties of linear alkyl benzene solvent,” *Chinese Phys. C* **40**, 016002 (2016), ISSN 1674-1137, <http://dx.doi.org/10.1088/1674-1137/40/1/016002>.

[17] H. Yang, *et al.*, “Light attenuation length of high quality linear alkyl benzene as liquid scintillator solvent for the JUNO experiment,” *J. Inst.* **12**, T11004 (2017), ISSN 1748-0221, <http://dx.doi.org/10.1088/1748-0221/12/11/T11004>.

[18] R. Zhang, *et al.*, “Using monochromatic light to measure attenuation length of liquid scintillator solvent LAB,” *NUCL SCI TECH* **30**, 30 (2019), ISSN 1001-8042, 2210-3147, <http://dx.doi.org/10.1007/s41365-019-0542-1>.

[19] D. Cao, *et al.*, “Light absorption properties of the high quality linear alkylbenzene for the JUNO experiment,” *Nuclear Instruments and Methods in Physics Research Section A: Accelerators, Spectrometers, Detectors and Associated Equipment* **927**, 230 (2019), ISSN 01689002, <http://dx.doi.org/10.1016/j.nima.2019.01.077>.

[20] “CAEN - Tools for Discovery,” <https://www.caen.it/>.

[21] M. Li, *et al.*, “Separation of scintillation and Cherenkov lights in linear alkyl benzene,” *Nuclear Instruments and Methods in Physics Research Section A: Accelerators, Spectrometers, Detectors and Associated Equipment* **830**, 303 (2016), ISSN 0168-9002, <http://dx.doi.org/10.1016/j.nima.2016.05.132>.

[22] Z. Guo, *et al.*, “Slow liquid scintillator candidates for MeV-scale neutrino experiments,” *Astroparticle Physics* **109**, 33 (2019), ISSN 0927-6505, <http://dx.doi.org/10.1016/j.astropartphys.2019.02.001>.

[23] S. Agostinelli, *et al.*, “Geant4—a simulation toolkit,” *Nuclear Instruments and Methods in Physics Research Section A: Accelerators, Spectrometers, Detectors and Associated Equipment* **506**, 250 (2003), ISSN 0168-9002, [http://dx.doi.org/10.1016/S0168-9002\(03\)01368-8](http://dx.doi.org/10.1016/S0168-9002(03)01368-8).

- [24] J. Allison, *et al.*, “Geant4 developments and applications,” IEEE Trans. Nucl. Sci. **53**, 270 (2006), ISSN 1558-1578, <http://dx.doi.org/10.1109/TNS.2006.869826>.
- [25] J. Allison, *et al.*, “Recent developments in Geant4,” Nuclear Instruments and Methods in Physics Research Section A: Accelerators, Spectrometers, Detectors and Associated Equipment **835**, 186 (2016), ISSN 0168-9002, <http://dx.doi.org/10.1016/j.nima.2016.06.125>.
- [26] T. K. Gaisser, R. Engel, and E. Resconi, *Cosmic Rays and Particle Physics* (Cambridge University Press, 2016).
- [27] M. Daimon and A. Masumura, “Measurement of the refractive index of distilled water from the near-infrared region to the ultraviolet region,” Appl. Opt., AO **46**, 3811 (2007), ISSN 2155-3165, <http://dx.doi.org/10.1364/AO.46.003811>.